

# Lawrence Berkeley National Laboratory

## Recent Work

### Title

Monte Carlo Simulations of Hydrophobic Polyelectrolytes. pH-Induced Structural Transitions for Polymers Containing Weak Electrolytes

### Permalink

<https://escholarship.org/uc/item/93d0n9xw>

### Authors

Beltran, S.

Sassi, A.P.

Hooper, H.H.

et al.

### Publication Date

1990-12-01



# Lawrence Berkeley Laboratory

UNIVERSITY OF CALIFORNIA

## Materials & Chemical Sciences Division

Submitted to Journal of Chemical Physics

### Monte Carlo Simulations of Hydrophobic Polyelectrolytes. pH-Induced Structural Transitions for Polymers Containing Weak Electrolytes

S. Beltrán, A.P. Sassi, H.H. Hooper, H.W. Blanch,  
and J.M. Prausnitz

December 1990



1 LOAN COPY 1  
1 Circulates 1  
1 for 2 weeks 1

Bldg. 50 Library.  
Copy 2

LBL-29988

## **DISCLAIMER**

This document was prepared as an account of work sponsored by the United States Government. While this document is believed to contain correct information, neither the United States Government nor any agency thereof, nor the Regents of the University of California, nor any of their employees, makes any warranty, express or implied, or assumes any legal responsibility for the accuracy, completeness, or usefulness of any information, apparatus, product, or process disclosed, or represents that its use would not infringe privately owned rights. Reference herein to any specific commercial product, process, or service by its trade name, trademark, manufacturer, or otherwise, does not necessarily constitute or imply its endorsement, recommendation, or favoring by the United States Government or any agency thereof, or the Regents of the University of California. The views and opinions of authors expressed herein do not necessarily state or reflect those of the United States Government or any agency thereof or the Regents of the University of California.

# MONTE CARLO SIMULATIONS OF HYDROPHOBIC POLYELECTROLYTES. pH-INDUCED STRUCTURAL TRANSITIONS FOR POLYMERS CONTAINING WEAK ELECTROLYTES

*Sagrario Beltrán\**, *Alexander P. Sassi*, *Herbert H. Hooper\*\**,  
*Harvey W. Blanch*, and *John M. Prausnitz\*\*\**

Chemical Engineering Department  
University of California

and

Chemical Sciences Division  
Lawrence Berkeley Laboratory  
Berkeley, CA 94720

## ABSTRACT

A Monte Carlo simulation method has been used to study the configurational properties of a cubic lattice-model for an isolated, partially ionized polyelectrolyte as a function of: (1) polymer hydrophobicity (2) fraction of ionizable segments (3) degree of dissociation of ionizable segments, and (4) Debye screening length. Together with the excluded volume, the polymer segments experience two other competing interactions: (1) intramolecular electrostatic interactions between ionized segments, calculated with a screened Debye-Hückel potential, and (2) non-electrostatic forces, represented by potential  $\epsilon$  which accounts for the net balance of short-range segment-segment, segment-solvent and solvent-solvent interactions. This model represents the main features of pH-sensitive, hydrophobic polyelectrolyte behavior in solution. Chain dimensions, calculated from this model, are qualitatively comparable to those obtained experimentally for pH-sensitive hydrophobic polyelectrolyte copolymer gels, as a function of copolymer composition, copolymer hydrophobicity, and pH or ionic strength of the solution surrounding the copolymer polyelectrolyte.

This work was supported by the Director, Office of Basic Energy Science, Chemical Sciences Division of the U.S. Department of Energy, under Contract Number DE-AC03-76SF 00098.

\* Present address: Departamento de Ingeniería Química, Colegio Universitario de Burgos, Universidad de Valladolid, 09002 Burgos, Spain

\*\*Present address: Air Products and Chemicals, Allentown, PA 18195

\*\*\* To whom correspondence should be addressed

submitted to: *Journal of Chemical Physics*, November 1990

## I. INTRODUCTION

Hydrophobic polymers and gels containing bound weak electrolytes undergo dramatic transitions in polymer structure (1-3) or gel volume (4) in response to changes in solution pH. At pH's where a large number of monomers are ionized, such polymers expand like polyelectrolytes; when the pH is such that few monomers are ionized, these polymers (or gels) collapse to condensed, hydrophobic conformations. The transformation from expanded to condensed conformations can be abrupt, and some evidence suggests the existence of a discontinuous, two-state transition.

Several factors may contribute to structural transitions in hydrophobic polyelectrolytes and gels. Manning (5) suggested that the onset of counterion condensation (at a critical chain charge density) triggers polymer structural rearrangement. Schwarz and Siegel (6) have proposed a theory for pH-induced gel-volume collapse based on the composition dependence of the dielectric constant within the gel, and the resulting effect of gel volume on the Born energy of hydration.

In an earlier paper (7), we presented Monte Carlo simulations which indicate that structural transitions in hydrophobic polyelectrolytes can result directly from the competition between coulombic repulsions and hydrophobic (segment-segment) attractions. In that work, large transitions were observed in the dimensions of a model polymer as the number of ionized groups on the chain increase; for highly hydrophobic chains, most of the change in structure occurred over a small range of chain ionization.

Variations in chain ionization have been modeled earlier (7) by changes in polymer chemical composition, i.e., the insertion or removal of ionized groups. Experimentally, transitions are typically observed for polymers or gels with *fixed* composition in response to variations in solution pH. In this paper we extend the model of Hooper et al. (7) to obtain a better approximation of the experimental conditions. We consider polyelectrolytes where the number of potentially ionizable groups is constant, but where the degree of dissociation of these groups depends on pH. We perform simulations in the canonical ensemble (constant  $N$ ,  $V$ ,  $T$ ) and the grand canonical ensemble (constant  $\mu$ ,  $V$ ,  $T$ ). In simulations performed in the canonical ensemble, the degree of dissociation is fixed at the outset of the simulation by one of two methods, as explained later. In simulations performed in the grand canonical ensemble, we fix the pH and the  $pK_a$  of the ionizable groups; the degree of

dissociation is allowed to find its equilibrium value. The resulting dependence of chain dimensions on degree of dissociation is mapped onto a pH scale.

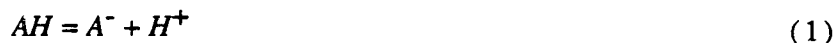
Hooper et al. (7) provide a basis for examining the effect of competing hydrophobic and hydrophilic (coulombic) interactions on polymer configurational properties. That study provides evidence for the occurrence of charge-induced structural transitions in hydrophobic polyelectrolytes. The study reported here investigates such transitions in a manner more directly analogous with that considered experimentally, and allows for qualitative comparison of simulation results with such experiments.

## II. MODEL AND SIMULATION METHOD

The model and simulation method used in this work are similar to those described in Ref. 7. We discuss here the general model features and the differences between this work and Ref. 7. The polymer is represented as a self-avoiding walk of  $N$  segments on a cubic lattice. In addition to excluded volume, the polymer segments experience short-range (non-electrostatic) and long-range (coulombic) interactions. Non-bonded nearest-neighbor segments interact with potential  $\epsilon$ ; we investigate here (as in Ref. 7)  $\epsilon < 0$ , i.e., the case where segment-segment contacts are energetically favored over segment-solvent contacts. We consider the favorable segment-segment interaction to be a result of polymer hydrophobicity. Thus, our model polymer is analogous to a polyelectrolyte containing hydrophobic (e.g., hydrocarbon) side groups. The hydrophobic groups tend to collapse the polymer, while the ionized groups work to expand the chain; the net result is a rich set of configurational properties, varying from collapsed to expanded structures depending on system conditions (7).

Ionized segments on the chain interact through screened coulombic repulsions. In Ref. 7, segments were either completely ionized (with a valence of unity) or uncharged. Ionized segments were evenly spaced along the chain, and the fraction of the total segments carrying charge,  $\lambda$ , varied from 0 to 1.0. In that work, changes in  $\lambda$  correspond to variations in polymer chemical composition; i.e., a series of chains with different  $\lambda$  are analogous to a series of copolymers containing different ratios of charged to uncharged monomer. There, the charged monomer is a strong electrolyte because its degree of dissociation remains constant with changes in solution conditions.

In this work we consider the effect of pH on the behavior of polyelectrolytes containing monomers or comonomers with weak electrolytes. We now define  $\lambda$  as the fraction of segments which are *potentially* ionizable, i.e., the fraction of comonomers containing weakly ionizable groups. We define  $\alpha$  as the *actual* ionization, i.e., the proportion of these groups which are dissociated. Considering the weakly ionizable groups to be acidic, the chemical equilibrium of interest (for a single monomer) is:



where  $AH$  is the undissociated monomer. If the equilibrium dissociation constant  $K_a$  is known, the relative proportion of undissociated to dissociated monomer can be determined as a function of solution pH according to:

$$\frac{[A^-][H^+]}{[AH]} = K_a \quad (2)$$

where  $[ ]$  denotes concentration, and the ratio of activity coefficients is assumed equal to unity.

Two problems arise in extending our model to weak electrolytes. First, dissociation constant  $K_a$  is typically known only for the *monomeric* species (if at all), and not for the monomer groups incorporated in the polymer chain (which are subject to a local environment different from that for the free monomers in solution). Second, assuming that we have an accurate expression for  $K_a$  for the monomers on the polymer, it is not obvious how best to include in the simulation the information contained in Eqn. (2) (e.g., the relative concentrations of  $AH$  and  $A^-$ ). Eqn. (2) describes a *time-averaged, dynamic* equilibrium where ionizable groups are protonated and deprotonated. In our simulations, the counterion in Eqn. (2) (hydrogen ion) is not included explicitly in the model. Furthermore, simulations in the canonical ensemble explore only configurational space ( $\alpha$  does not vary during the simulation), whereas simulations in the grand canonical ensemble allow  $\alpha$  to fluctuate. Initially we assume that  $K_a$  for the polymeric groups is known, and we consider the second problem. In the next section we return to the first problem.

We consider first simulations in the canonical ensemble, which can be shown to be equivalent to simulations in the mean-field sense. We have considered two methods for incorporating the dissociation equilibrium of Eqn. (2) in our simulation

model. In both methods, we define  $\alpha$  as the degree of dissociation of the ionizable groups. For the example of a weak acid (discussed above), we have

$$\alpha = \frac{[A^-]}{[AH] + [A^-]} \quad (3)$$

When  $\alpha=0$ , all segments on the polymer are uncharged and we reach the well-studied limit of an attractive self-avoiding walk. When  $\alpha=1$ , all ionizable segments (i.e., the fraction  $\lambda$  of the total number of segments) are dissociated, and we obtain the limit studied in Ref. 7. Now we consider conditions between those two limits. In the first method, we average the dissociation equilibria of Eqn. (1) over both time and monomer position; thus, the charge on the ionizable monomer is constant throughout the simulation, and is independent of monomer location. This method requires allowing monomers to have *fractional ionizations* which are equal to the degree of dissociation  $\alpha$ ; i.e., the charge on monomer  $i$  (for a given  $\alpha$ ) is:

$$q_i = \alpha z_i e \quad (4)$$

where  $z_i$  is the valence of segment  $i$  in the fully dissociated state (1 for ionizable segments and 0 for other segments) and  $e$  is the electronic charge.

In the second method, we allow the averaging process to occur during the course of a simulation. Ionizable monomers are either completely ionized (dissociated) or uncharged (associated); the fraction of a simulation run that an ionizable monomer spends in the dissociated state is equal to its degree of dissociation,  $\alpha$ . This averaging is accomplished by reapplying the equilibrium criterion of Eqn. (2) to *each* ionizable monomer after every 500 simulation steps. For each ionizable monomer, a random number between 0 and 1 is generated and compared with  $\alpha$ . If the number is greater than  $\alpha$ , the group is uncharged for the next 500 simulation steps; if the number is less than  $\alpha$ , the group is ionized (with a valence  $z$ ) for the next 500 simulation steps. For a given simulation, all ionizable monomers have the same  $\alpha$ , and thus spend the same *average* fraction of the simulation run ionized. However, at any given point in the simulation, the dissociation equilibrium of each ionizable monomer is independent of the other monomers.

For simulations using the above two methods, the ionization  $\alpha$  is predetermined by applying Eq. (2) for a given pH and does not vary during the simulation.



However, in an equilibrium experiment such as Siegel's gel-swelling experiments, the ionization is not known *à priori*. Instead, the pH is fixed for the duration of the experiment. Because fixing pH is equivalent to fixing the chemical potential of the hydrogen ion, grand canonical simulations (constant  $\mu$ ,  $V$ ,  $T$ ) mimic the experiment more closely. In simulations in the grand canonical ensemble, the ionization  $\alpha$  fluctuates; therefore, the energetics of protonating or deprotonating an ionizable group depend on the local environment surrounding the ionizable group.

Because of the possible presence of a phase transition in the chain, it can be debated whether the results of the simulation should be independent of the ensemble in which it is performed. We therefore performed simulations in the grand canonical ensemble to determine if local fluctuations in  $\alpha$  are significant at this level of simulation.

In the grand canonical simulation, the pH and  $pK_a$  are fixed at the outset of the simulation. As in the second method discussed above, ionizable monomers are either completely ionized (dissociated) or uncharged (associated). After every 100 simulation steps, one of the potentially ionizable groups is selected at random. If the selected group is neutral, the group becomes ionized, and vice-versa. In such a manner, the ionization  $\alpha$  is allowed to reach its equilibrium value.

In the remaining portion of this section we describe the simulation as applied to the three methods discussed above. In the following section we compare results of the three methods, and discuss potential implications of any differences on the goals and conclusions of this work.

The configurational energy for the chain is a sum of electrostatic and non-electrostatic (dispersion-force) contributions:

$$E = E_{el} + E_{nel} \quad (5)$$

The non-electrostatic energy is

$$E_{nel} = \epsilon m \quad (6)$$

where  $m$  is the total number of contacts between non-bonded nearest neighbor segments. The electrostatic energy is the sum over long-range coulombic interactions between all pairs of ionized segments:

$$E_{el} = \sum_i^{N-1} \sum_{j=i+1}^N u_{ij} \quad (7)$$

Where  $N$  is the number of segments in the chain and  $u_{ij}$  is given by a screened Debye-Hückel coulombic potential (8):

$$u_{ij} = \frac{q_i q_j}{D r_{ij}} \exp(-\kappa r_{ij}) \quad (8)$$

where segments  $i$  and  $j$  carry charge  $q_i$  and  $q_j$  respectively, and are separated by a distance  $r_{ij}$ . The dielectric constant  $D$  is that of water at 25°C. The charges on segments  $i$  and  $j$  are determined as described above. The inverse Debye screening length  $\kappa$  is given by (8):

$$\kappa^2 = \frac{4 \pi e^2 N_A \sum_i z_i C_i}{D k T} \quad (9)$$

where  $N_A$  is Avogadro's number,  $C_i$  is the concentration of ionic species  $i$ ,  $k$  is Boltzmann's constant, and  $T$  is the temperature. We consider the polyelectrolyte at infinite dilution; thus, the sum in Eqn. (9) is over the species of *added* electrolyte, and does not include the charges on the polymer or the counterions. For convenience, in the discussion of results we assume that the added electrolyte is a 1:1 salt, and we refer either to the Debye screening length,  $\kappa^{-1}$ , or to the concentration of added electrolyte ( $C_i$ ) which results in that screening length.

Polyelectrolyte configurational properties were calculated using the Metropolis Monte-Carlo method (9). The chain is initially placed in a three-dimensional staircase configuration; successive configurations are generated by combination of elementary chain movements. Both *reptation* (10) and *internal* chain movements are used as discussed by Hooper et al. (7) In the canonical ensemble, new configurations are accepted based on the probability:

$$p_{s+1} = \min\{1, \exp(-\Delta E/kT)\} \quad (10)$$

where  $\Delta E$  is the energy change in going from configuration  $s$  to configuration  $s+1$ . In the grand canonical ensemble, new configurations are accepted based on the probability (for a weak base):

$$p_{s+1} = \min\{1, \exp\{(-\Delta E/kT) + \Delta m_c(pK_a - pH)\ln 10\}\} \quad (11)$$

where  $\Delta E$  is as above and  $\Delta m_c$  is the change in number of ionized groups in going from configuration  $s$  to configuration  $s+1$ . The term  $\exp\{m_c(pK_a - pH)\ln 10\}$  expresses the probability that the chain has  $m_c$  charges based on Eq. (2) for a given configuration.

Trial configurations which result in a reduced or uncharged energy (i.e.,  $\Delta E \leq 0$ ) are always accepted. Configurations which increase the chain energy are accepted with probability  $\exp(-\Delta E/kT)$  in the canonical ensemble and with probability  $\exp\{(-\Delta E/kT) + \Delta m_c(pK_a - pH)\ln 10\}$  in the grand canonical ensemble.

The chain is initially relaxed through  $5 \times 10^4$  attempted movements (cycles); configurational properties are calculated (and recorded) every  $10^4$  cycles. This sampling frequency was found sufficient to generate statistically uncorrelated configurations for the 40-segment chains studied here. A total of 200 configurations are sampled for each run, requiring  $2 \times 10^6$  Monte-Carlo cycles. The property of primary interest here is the size of the polymer coil, characterized by its mean-square end-to-end distance:

$$\langle r^2 \rangle = \langle (r_n - r_1)^2 \rangle \quad (11)$$

and its mean-square radius-of-gyration:

$$\langle s^2 \rangle = \frac{1}{N} \left\langle \sum_{i=1}^N (r_i - r_{cm})^2 \right\rangle \quad (13)$$

where  $r_i$  is the position vector locating the  $i$ th chain segment,  $r_{cm}$  is the vector locating the chain center of mass, and  $\langle \rangle$  denotes an average over the 200 samples in a Monte-Carlo run. These properties are reported here as reduced variables;  $\langle r^2 \rangle$  is reduced by the value it would have in a fully extended configuration,  $(N-1)^2 l^2$ , and  $\langle s^2 \rangle$  is reduced by  $(N-1)l^2$ .

### III. RESULTS AND DISCUSSION

Configurational properties were calculated for 40-segment chains as a function of polymer hydrophobicity ( $\epsilon/kT$ ), fraction of segments which are ionizable ( $\lambda$ ), the degree of dissociation of these ionizable segments ( $\alpha$ ), and the Debye screening length ( $\kappa^{-1}$ ). Varying independently all four parameters would require a needlessly large amount of computation, unnecessary for the goals of this work. We observed in Ref. 7 the qualitative behavior of model polyelectrolytes with competing hydrophobic and coulombic interactions. Our goal here is to provide a basis for comparing (qualitatively) simulation results with pH-induced transitions seen for real hydrophobic polyelectrolytes. Thus, system parameters were varied in analogy to two sets of experiments performed by Siegel and Firestone (4) for hydrophobic polyelectrolyte copolymer gels. Siegel and Firestone studied a series of (dimethylamino)ethyl methacrylate (DMA) / n-alkyl methacrylate ester (n-AMA) copolymer gels in which the DMA is the ionizable monomer, and the n-alkyl chain length in the n-alkyl methacrylate ester is varied to vary the gel hydrophobicity. We vary the number of ionizable groups,  $\lambda$ , in our model polyelectrolyte chain to simulate the variation of percentage of ionizable comonomer, the degree of ionization of such groups to simulate the variation in pH, and the non-electrostatic interactions  $\epsilon/kT$  to simulate the hydrophobicity of the gel. Siegel and Firestone measured the gel swelling capacity in buffer solutions and we calculate the analogous configurational property, (i.e., end-to end distance) to calculate the dimensions of our model polyelectrolyte chain in solutions of different ionic strength.

Before undertaking a comparison with experimental data, we first consider the general system behavior and the differences among the three models used here. For purposes of this (and the following) discussion, we must transform the variable  $\alpha$  into pH coordinates for results obtained in canonical-ensemble simulations. This mapping can be performed with Eqns. (2) and (3) once we specify a  $K_a$  for the ionizable groups on the polymer. Because we will be considering the experimental data of Siegel and Firestone (4), we consider our ionizable monomer to be DMA, and we use the value for the dissociation constant of protonated DMA given in Ref. 4 as  $pK_a=7.7$ .

Figure 1 presents (for all models) the dependence of the reduced end-to-end distance on pH for chains with a constant composition of ionizable comonomer

( $\lambda=0.325$ ) and varying hydrophobicity ( $-1.5 \leq \epsilon/kT \leq 0$ ). Because the ionizable monomers are weakly basic (DMA), these monomers are charged at pH's lower than  $pK_a$ , and uncharged at pH's higher than  $pK_a$ . Thus, the chains expand at low pH, and condense to more compact configurations at high pH. The transformation between the two regimes is fairly abrupt (though clearly continuous), and is centered around the  $pK_a$  of 7.7.

The transformation of chain dimensions as a function of pH seen in Figure 1 for *weakly dissociating* polyelectrolytes is analogous to the charge-induced structural transitions reported in Ref. 7 for *strongly dissociating* polyelectrolytes. The pH scale in Figure 1 provides a measure of total chain ionization; therefore, it is not surprising that our results are similar to those in Ref. 7. The difference here is that we can translate (or map) the variation in polymer charge onto a pH scale. The particular choice of  $pK_a$  (and whether the ionizable monomer is acidic or basic) affects only the location (and direction) of the structural transitions, and not their shapes or magnitudes; thus,  $pK_a$  can be considered a transformation variable which quantifies the coordinate mapping.

We now consider differences in results for the three methods used for approximating the ionization equilibria. We denote as *Model 1a* the canonical-ensemble case where fractional ionizations are used; as *Model 1b* the canonical-ensemble case where the averaging occurs independently for each ionizable monomer during simulation; and as *Model 2* the case performed in the grand canonical ensemble, where  $\alpha$  fluctuates during simulation. Figure 1 shows that the three models yield closely similar results over the entire pH (degree-of-dissociation) range; however, Model 1a always gives slightly larger end-to-end distances than Model 1b and Model 2. The difference between Models 1a and 1b is largest in the transition region, where end-to-end distances for Model 1a are as much as 20-30% larger than those for Model 1b. Remote from the transition, differences in Models 1a and 1b become smaller; these differences disappear when the two models become identical at the extremes  $\alpha=0$  and  $\alpha=1$ . Model 2 gives the same results (within one standard deviation) as Model 1b.

Why do we observe differences between Models 1a and 1b, and why are these differences always in the direction of more expanded conformations for Model 1a? A possible explanation is that the charges in Model 1a are spaced closer along the chain than in Model 1b (because all ionizable groups in Model 1a have the same fractional charge); this closer spacing between charged groups results in increased electrostatic repulsions which tend to expand the polymer. However, neither Model

1a nor Model 1b provides an exact representation of the real (dynamic) dissociation equilibria for a weak electrolyte; instead, both models are attempts at approximating the *effect* of these equilibria.

Of the three simulation methods, Model 2 intuitively provides the most realistic model; pH is held constant, and  $\alpha$  is allowed to fluctuate about its equilibrium value. Models 1a and 1b are in the mean-field limit. Deviations of mean-field-predicted behavior from realistic behavior would be expected to be largest in the region near a phase transition. Evidence supporting the occurrence of a phase transition near  $\text{pH} = \text{p}K_a$  is shown in Figure 2, which shows the dependence of the heat capacity,  $C_v$ , on pH for a chain where  $\lambda=0.325$ ,  $\epsilon/kT = -1.0$ , and  $\kappa^{-1}=96.2 \text{ \AA}$ . The peak in the heat capacity between pH 7-8 indicates the existence of a phase transition between an extended and a collapsed state.

Simulations were performed using Model 2 over the extremes of  $\lambda$ ,  $\epsilon/kT$ , and  $\kappa^{-1}$  explored with Model 1b; in all cases, agreement was virtually exact. Furthermore, the ionization  $\alpha$  predicted by Model 2 as a function of pH matched that used for Model 1b simulations. This means that the mean-field approximation (i.e., simulation in the canonical ensemble) is valid for simulating configurational behavior near the phase transition for the ranges of parameters studied here.

Given the agreement between simulations in the canonical and grand canonical ensemble and the (relatively) small deviations between Model 1a and Model 1b, the choice of one model over another for the remainder of the discussion (which encompasses the main goal of this work) will not affect the outcome of this discussion. In the following (qualitative) comparison of simulation with experiment, we present results from Model 1b.

In the first set of simulations, we consider a series of polymers of constant content of ionizable groups ( $\lambda=0.325$ ), and of varying hydrophobicity ( $\epsilon/kT$ ). Configurational properties for this series of model polymers are calculated as a function of the degree of dissociation  $\alpha$  for  $\kappa^{-1}=9.62 \text{ \AA}$  (Fig. 2) and for  $\kappa^{-1}=96.2 \text{ \AA}$  (Fig. 1). This set of simulations is qualitatively analogous to the swelling experiments of Siegel and Firestone (4) for a series of DMA / n-alkyl methacrylate ester (n-AMA) copolymer gels in which the DMA (ionizable monomer) content is held constant, and the n-alkyl chain length (hydrophobicity) is varied. In that work, swelling equilibria were measured as a function of pH at 0.1M total ionic strength (Figure 3b). Figure 3a shows the dependence of the end-to-end distance on pH (as calculated from DMA dissociation,  $\text{p}K_a=7.7$ ) and on polyelectrolyte hydrophobicity for  $\kappa^{-1}=9.62 \text{ \AA}$  (ionic strength 0.1M). Siegel and Firestone employed gels containing 30% mol DMA

in the set of experimental results shown in Figure 3b. To compare calculated and experimental results, we consider the number of ionizable groups in the chain equal to 32.5%, which is as close to 30% we can have without changing the charge distribution in the model. The transition from extended to collapsed chains in Fig. 3a occurs at lower pH's for highly hydrophobic polyelectrolytes (i.e.,  $\epsilon/kT=-1.5$ ) than for non-hydrophobic polyelectrolytes (i.e.,  $\epsilon/kT=0$ ) and the magnitude of this transition decreases with increasing hydrophobicity. Fig 3a shows that we observe higher collapsed configurations for highly hydrophobic chains than for non-hydrophobic chains not only in the extended state (low pH) but also in the collapsed state (high pH). The same qualitative features were found by Siegel and Firestone in their experiments with polyelectrolyte copolymer gels of varying hydrophobicity (Figure 3b). The main difference between the experimental and Monte Carlo results lies in the nature of the transition from stretched to collapsed configurations. While Firestone and Siegel see evidence for a discontinuous transition, in Monte-Carlo results, this transition is clearly continuous.

The results shown in Fig. 1 represent the dependence of the end-to-end distance on pH (as calculated from DMA dissociation,  $pK_a=7.7$ ) and on polyelectrolyte hydrophobicity for  $\kappa^{-1}=96.2 \text{ \AA}$  (ionic strength 0.001M). The difference between Figures 3a and 1 is the ionic strength where the end-to-end distances have been calculated; by comparing both figures, we can see that an increase in the ionic strength screens the electrostatic forces and impedes the chain to adopt highly extended configurations.

In the second set of simulations, we consider a series of polymers of constant hydrophobicity ( $\epsilon/kT$ ), but varying  $\lambda$  (i.e., varying content of ionizable groups). As in the first case, configurational properties were calculated as a function of  $\alpha$  for  $\kappa^{-1}=9.62 \text{ \AA}$  (Fig. 4a) and for  $\kappa^{-1}=96.2 \text{ \AA}$  (Fig. 5), i.e., for 1:1 electrolyte concentrations of 0.1 and 0.001M. This set of simulations is qualitatively analogous to the swelling measurements of Siegel and Firestone (4) for a series of copolymer methyl methacrylate (MMA) / (dimethylamino)ethyl methacrylate (DMA) gels. Siegel and Firestone measured swelling equilibria as a function of pH for gels of varying DMA (ionizable comonomer) content at 0.1M total ionic strength. Figure 4a shows the dependence of the end-to-end distance on pH (as calculated for dissociation of DMA,  $pK_a=7.7$ ) and on chain content of ionizable groups (DMA) for an ionic strength of 0.1 and non-electrostatic pair potential ( $\epsilon/kT=-0.5$ ). Fig. 4a indicates that our model clearly represents the decrease of the end-to-end distance with the number of ionizable groups, and dissociated ionizable groups. Siegel and Firestone (Fig. 4b)

report a displacement of the transition (from expanded to collapsed gels) to lower pH's when the content of ionizable groups,  $\lambda$ , decreases. In our simulations we find the same qualitative trend for this displacement.

Figure 5 shows the dependence of the end-to-end distance on pH (as calculated for dissociation of DMA,  $pK_a=7.7$ ) and on chain content of ionizable groups (DMA) for ionic strength of 0.001 and non-electrostatic pair potential ( $\epsilon/kT=-0.5$ ). The results shown in Fig. 5 are qualitatively similar to those represented in Fig. 4; however, the end-to-end distances are larger when the ionic strength is 0.001 M (Fig. 5); since the electrostatic forces are not as effectively screened as when the ionic strength is 0.1 M (Fig. 4), the repulsion between equal charged segments promotes highly extended configurations.

Figures 6a and 7 show the dependence of the end-to-end distance on pH (as calculated for dissociation of DMA,  $pK_a=7.7$ ) and on chain content of ionizable groups (DMA) for ionic strengths of 0.1M and 0.001M respectively. The non-electrostatic pair potential is  $\epsilon/kT=-1.0$  in both figures. The results shown in Fig. 6a can be compared to those of Fig. 6b (reproduced from Siegel and Firestone (4)) which represent the swelling isotherms as a function of pH for the n-butyl methacrylate (BMA) / DMA copolymers at various ionizable comonomer (DMA) compositions. Our model indicates the decrease of chain dimensions and the shift of the dimension transitions to lower pH's as the number of ionized groups increases. Siegel and Firestone studied the variation of hydrophobicity in their gels by varying the hydrophobic comonomer from MMA to BMA. We studied the same type of variation by varying the hydrophobicity  $\epsilon/kT$ , from  $\epsilon/kT=-0.5$  to  $\epsilon/kT=-1.0$ . This variation of hydrophobicity is not intended to be quantitatively comparable in both cases. However, comparing the results obtained for a hydrophobic polyelectrolyte  $\epsilon/kT=-1.0$  with the results for a less hydrophobic polyelectrolyte (i.e.,  $\epsilon/kT=-0.5$ ), shows that the chain dimensions are smaller for the more hydrophobic polyelectrolyte for all polyelectrolyte ionizations,  $\alpha$ , (or for all pH's). Similarly, BMA/DMA gels do not swell as much as MMA/DMA gels, due to the higher hydrophobicity of the butyl group compared with that of the methyl group in the non-ionizable comonomers.

#### IV. CONCLUSIONS

Configurational properties were calculated for 40-segment chains as a function of polymer hydrophobicity ( $\epsilon/kT$ ), fraction of ionizable segments, ( $\lambda$ ), degree of



dissociation of these ionizable segments ( $\alpha$ ), and Debye screening length ( $\kappa^{-1}$ ). Monte Carlo simulations were obtained for a cubic-lattice model of an isolated, partially ionized polyelectrolyte. Along with the excluded volume, the polymer segments experience two other competing interactions: (1) intramolecular electrostatic interactions between ionized segments, calculated with a screened Debye-Hückel potential, and (2) non-electrostatic forces, represented by the potential  $\epsilon$ ; this potential accounts for short-range segment-segment, segment-solvent and solvent-solvent interactions. Our model represents the main features of pH-sensitive, hydrophobic polyelectrolyte behavior in solution. When varying copolymer composition, copolymer hydrophobicity, pH or ionic strength of the solution surrounding the copolymer polyelectrolyte, calculated chain dimensions are qualitatively comparable to experimental results for pH-sensitive hydrophobic polyelectrolyte copolymer gels.

#### ACKNOWLEDGMENTS

This work was supported by the Director, Office of Energy Research, Office of Basic Energy Sciences, Chemical Sciences Division of the U.S. Department of Energy under contract No. DE-AC03-76SF00098. A.S. is grateful to the National Science Foundation for a pre-doctoral fellowship, and S.B. is grateful to the Spanish Ministry of Education and Science (MEC) for a post-doctoral fellowship. The calculations reported here were performed on the IBM 3090 at the U.C. Berkeley Computing Center; we acknowledge with thanks the generous computation time provided by the Computing Center. The authors are grateful to David Chandler, Ronald Siegel and Doros Theodorou for helpful comments and suggestions.

## REFERENCES

1. P. L. Dubin and U. P. Strauss, *J. Phys. Chem.* **74**, 2842 (1970).
2. U. P. Strauss, B. W. Barbieri and G. Wong, *J. Phys. Chem.* **83**, 2840 (1979).
3. U. P. Strauss, *Macromolecules* **15**, 1567 (1982).
4. R. A. Siegel and B. A. Firestone, *Macromolecules* **21**, 3254 (1988).
5. G. S. Manning, *J. Phys. Chem.* **89**, 3772 (1988).
6. B. Schwarz and R.A. Siegel, work in preparation.
7. H. H. Hooper, S. Beltran, A. P. Sassi, H. W. Blanch and J. M. Prausnitz, *J. Chem. Phys.* **93**, 2715 (1990).
8. P.H. Rieger, *Electrochemistry*, Prentice Hall, Inc., (1987).
9. N. Metropolis, A. W. Rosenbluth, M. N. Rosenbluth, A. H. Teller and E. Teller, *J. Chem. Phys.* **21**, 1087 (1953).
10. F. T. Wall and F. Mandel, *J. Chem. Phys.* **63**, 4592 (1975).

## Figure Captions

**Figure 1.** Dependence of the reduced end-to-end distance, calculated according to the two models studied in this work, on pH (as calculated for dissociation of DMA,  $pK_a=7.7$ ) for chains with a constant composition of ionizable segments ( $\lambda=0.325$ ) and varying hydrophobicity ( $-1.5 \leq \epsilon/kT \leq 0$ ). The ionic strength is 0.001M in all cases. Void symbols along with dashed lines represent Model 1a, full symbols along with continuous lines represent Model 1b, and small, open symbols with dotted lines represent Model 2.

**Figure 2.** Dependence of the heat capacity of the chain on pH for a chain with  $\lambda=0.325$ ,  $\epsilon/kT = -1.0$ , and  $pK_a=7.7$ . Ionic strength is held at 0.001 M. Both Model 1b (canonical ensemble) and Model 2 (grand canonical ensemble) give the same results. The peak in heat capacity indicates the occurrence of a phase transition.

**Figure 3.** (a) Dependence of the end-to-end distance on pH (as calculated for dissociation of DMA,  $pK_a=7.7$ ) for chains with a constant composition of ionizable segments ( $\lambda=0.325$ ) and varying hydrophobicity ( $-1.5 \leq \epsilon/kT \leq 0$ ). The ionic strength is 0.1M in all cases. (b) Swelling isotherms for a series of n-AMA/DMA copolymers of various side-chain lengths measured as a function of pH at 25°C and a total ionic strength of 0.1M. Each copolymer contained 30 mol % DMA. (♦) MMA/DMA; (▼) EMA/DMA; (■) PMA/DMA; (○) BMA/DMA; (□) HMA/DMA.

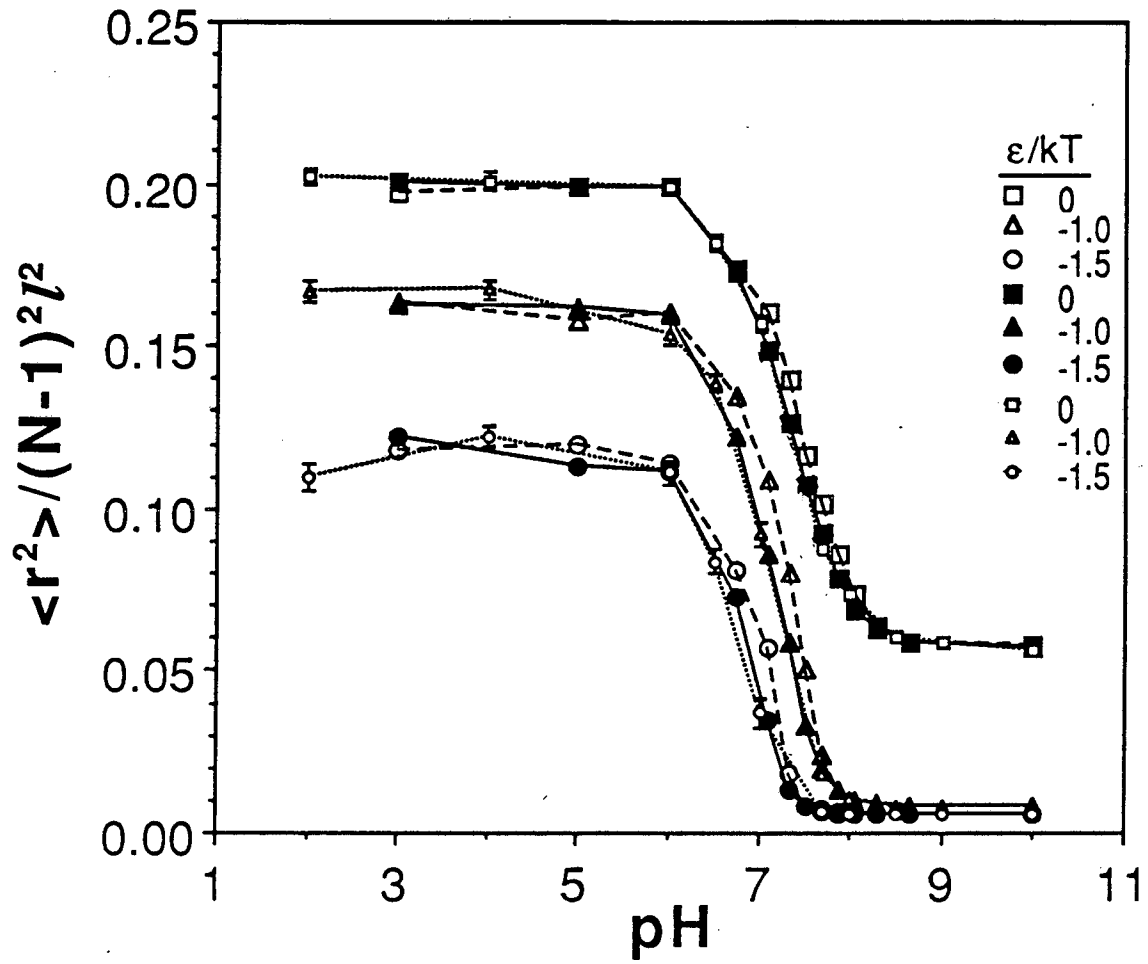
**Figure 4.** (a) Dependence of the end-to-end distance on pH (as calculated for dissociation of DMA,  $pK_a=7.7$ ) and on chain content of ionizable groups (DMA) for an ionic strength of 0.1M and non-electrostatic pair potential  $\epsilon/kT=-0.5$ . (b) Swelling isotherms for the MMA/DMA copolymers of various comonomer composition measured as a function of pH at 25°C and a total ionic strength of 0.1M. (■) 70/30 mol %; (●) 78/22 mol %; (▲) 86/14 mol %; (◆) 93/7 mol %.

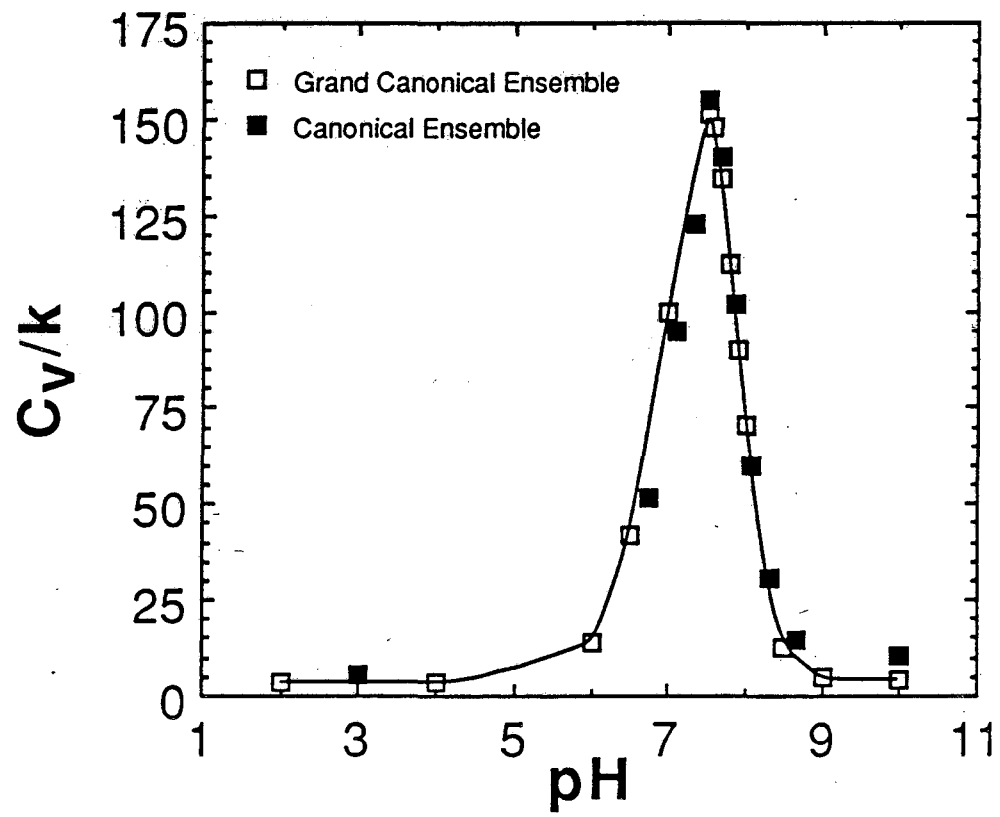
**Figure 5.** Dependence of the end-to-end distance on pH (as calculated for dissociation of DMA,  $pK_a=7.7$ ) and on chain content of

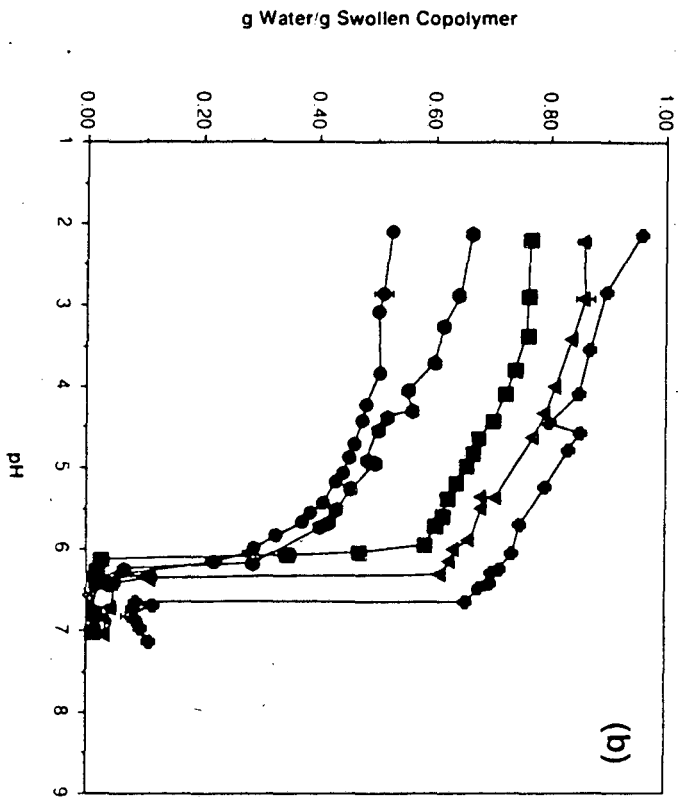
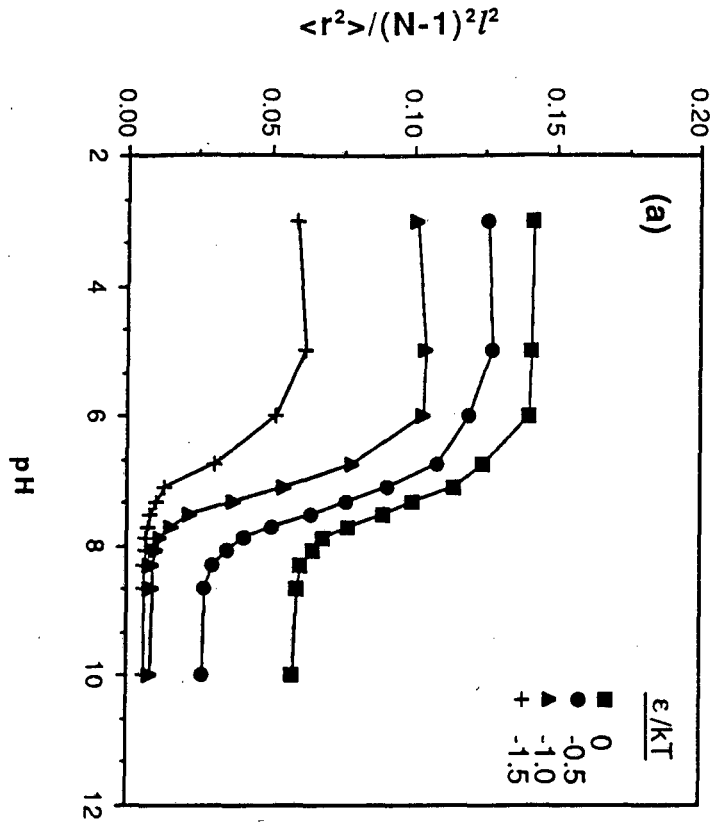
ionizable groups (DMA) for ionic strength of 0.001M and non-electrostatic pair potential  $\epsilon/kT=-0.5$ .

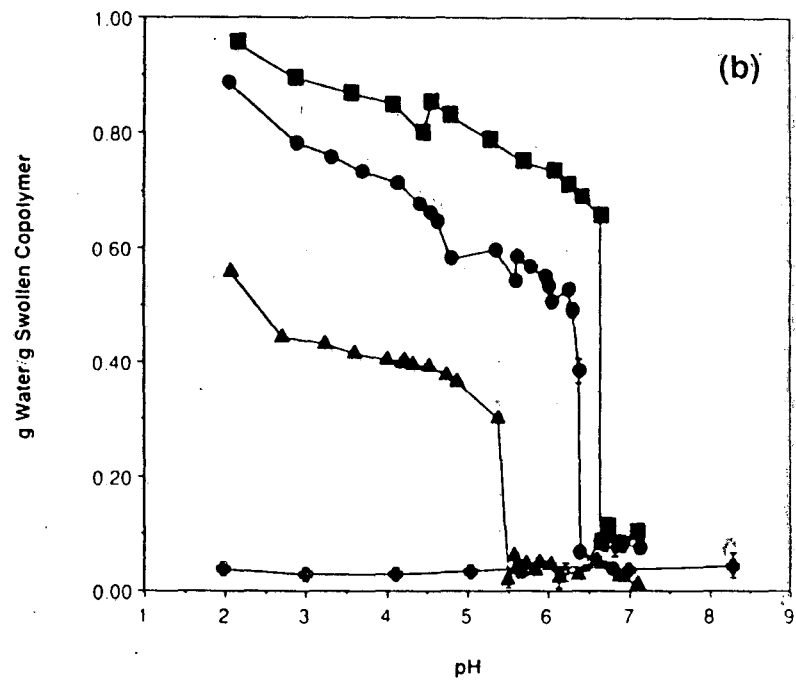
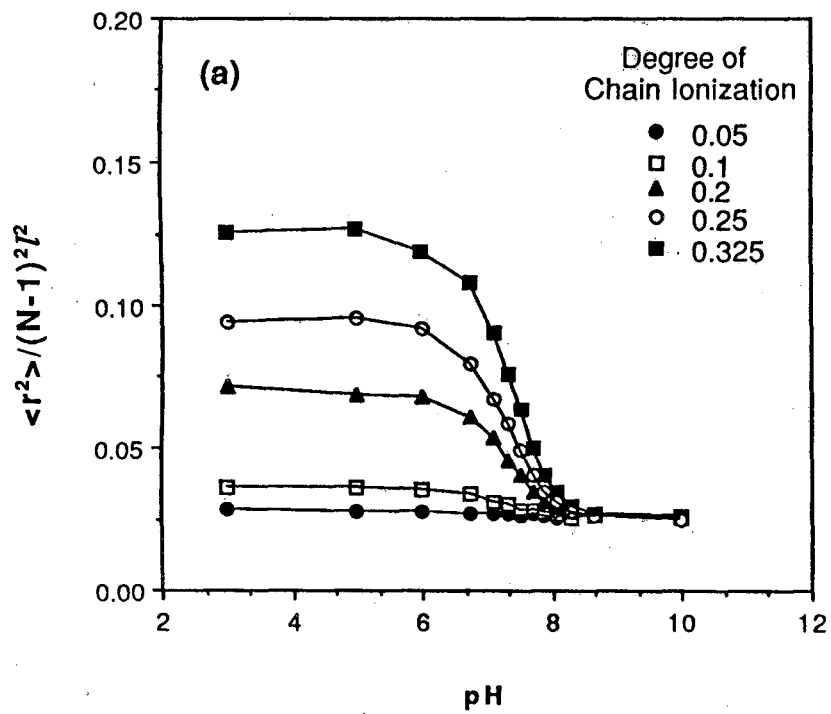
**Figure 6.** (a) Dependence of the end-to-end distance on pH (as calculated for dissociation of DMA,  $pK_a=7.7$ ) and on chain content of ionizable groups (DMA) for ionic strength of 0.1M and non-electrostatic pair potential  $\epsilon/kT=-1.0$ . (b) Swelling isotherms for the BMA/DMA copolymers of various comonomer composition measured as a function of pH at 25°C and a total ionic strength of 0.1M. (●) 70/30 mol %; (■) 77/23 mol %; (▲) 86/14 mol %.

**Figure 7.** Dependence of the end-to-end distance on pH (as calculated for dissociation of DMA,  $pK_a=7.7$ ) and on chain content of ionizable groups (DMA) for ionic strength of 0.001M and non-electrostatic pair potential  $\epsilon/kT=-1.0$ .

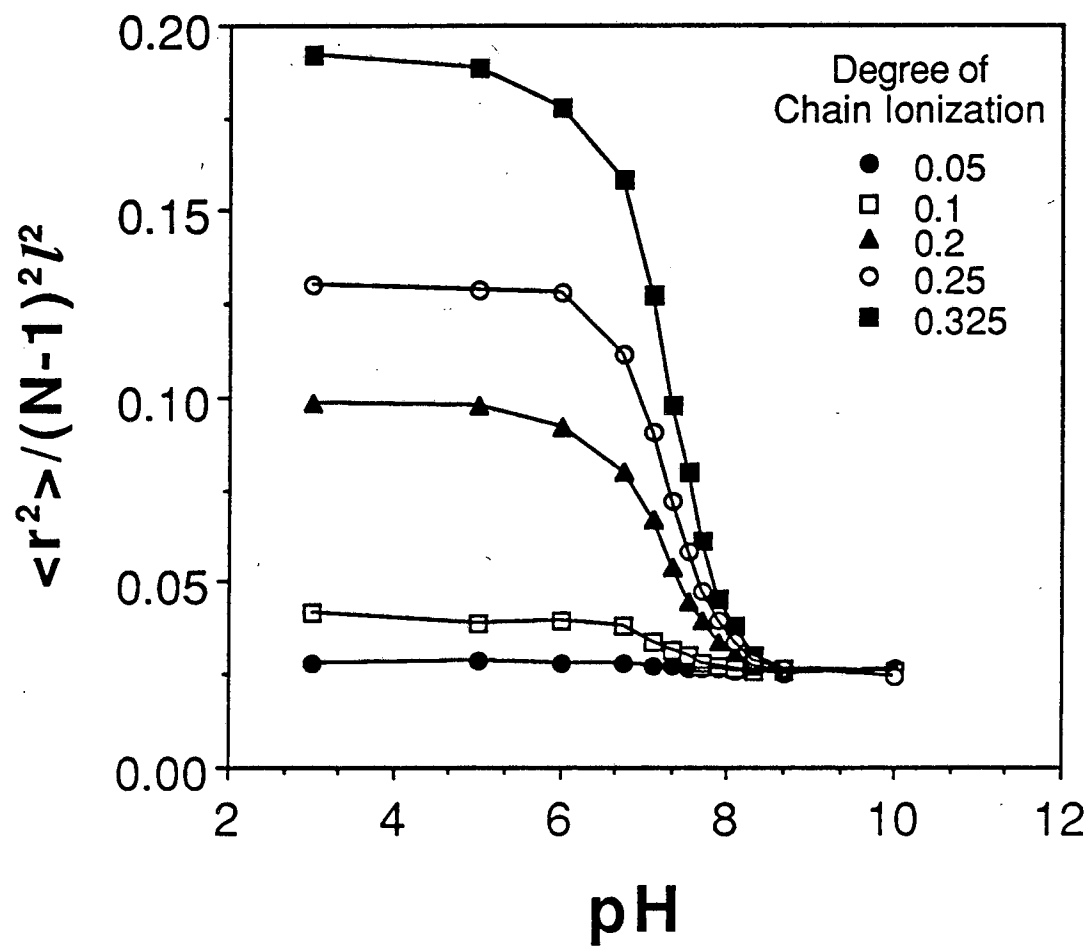


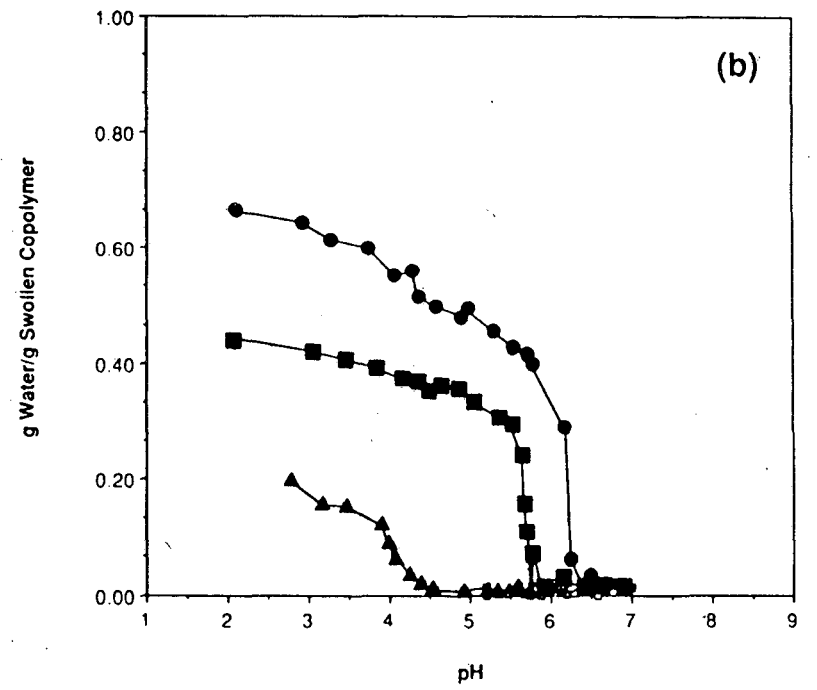
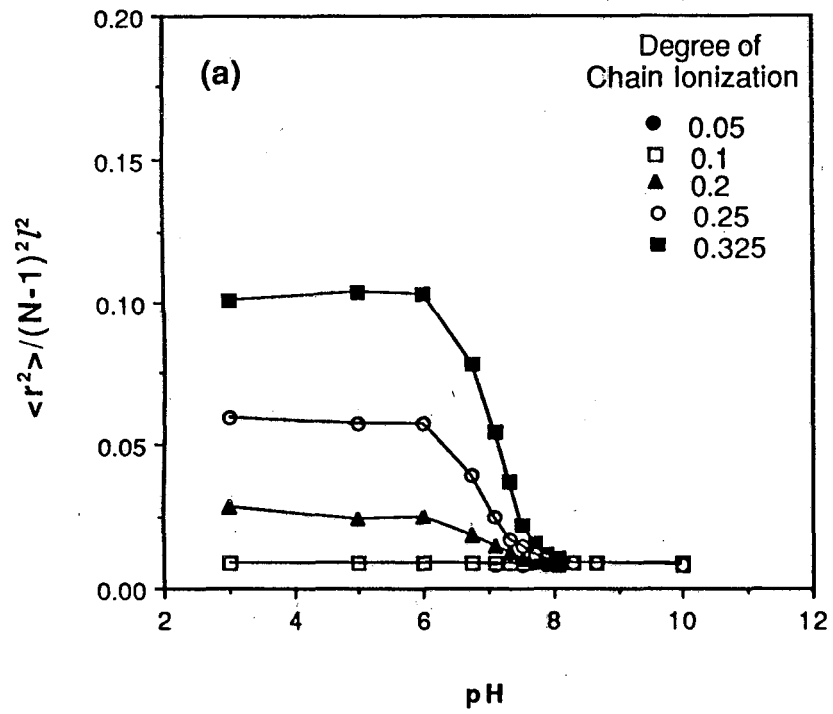


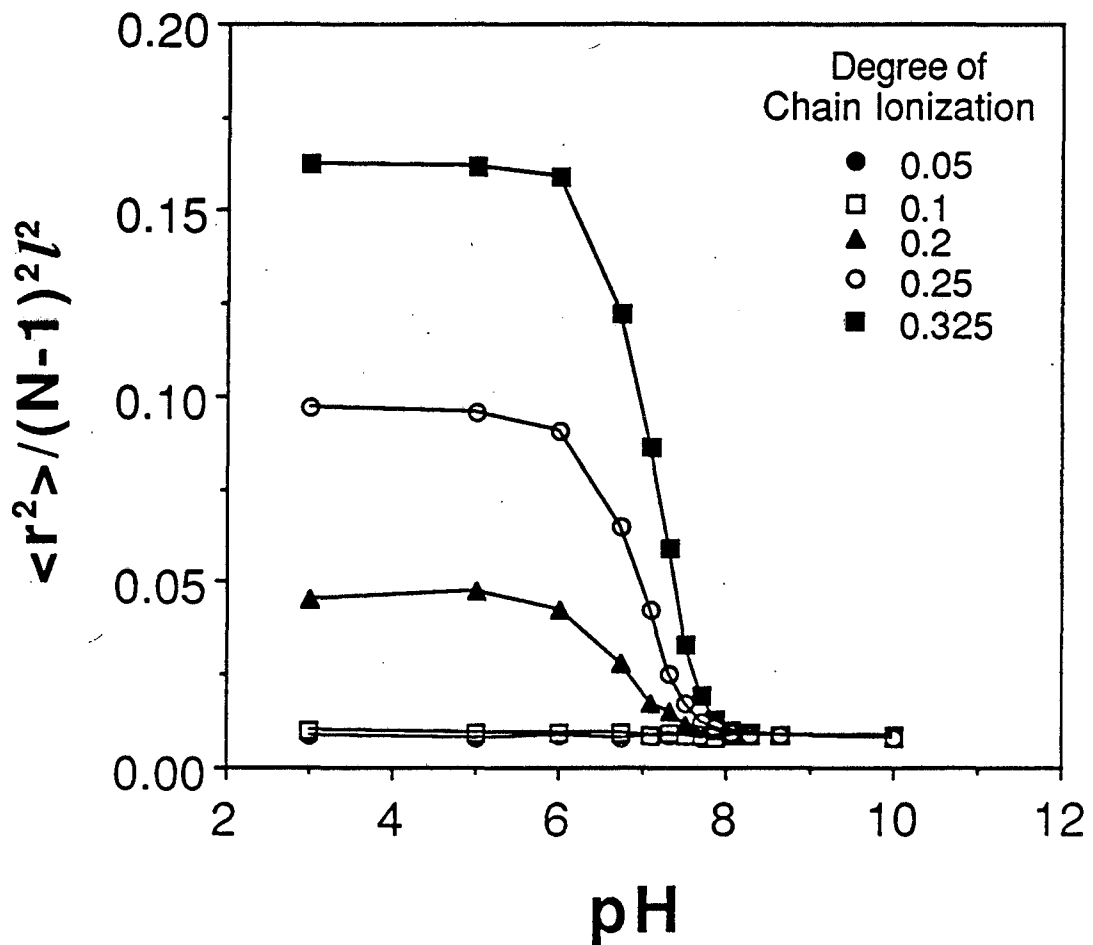












LAWRENCE BERKELEY LABORATORY  
UNIVERSITY OF CALIFORNIA  
INFORMATION RESOURCES DEPARTMENT  
BERKELEY, CALIFORNIA 94720